Journal of Sol-Gel Science and Technology
https://doi.org/10.1007/s10971-023-06190-y

ORIGINAL PAPER

Ammonia and nitrogen dioxide detection using ZnO/CNT nanocomposite synthesized by sol–gel technique

Saad Abbas Jasim[1] · Hikmat A. J. Banimuslem[2] · Forat H. Alsultany[3] · Ehssan Al-Bermany[1] · Rawaa M. Mohammed[3]

Received: 1 June 2023 / Accepted: 11 July 2023

Abstract

Through the use of sol–gel method, a composite material was created based on zinc oxide (ZnO) and multi-walled carbon nanotubes (CNT). As evidenced by the color of the solution and SEM images, colloidal nanoparticles were produced. For the construction of the devices, thin layers were deposited utilizing the spray pyrolysis on glass substrates and interdigitated electrodes. Samples were heated at different annealing temperatures ranging from 200 to 400 °C. The samples heated at 400 °C, have shown better interaction between zinc oxide and carbon nanotubes and achieved the sensitivity goal. Utilizing Tauc calculations and UV–visible absorption spectroscopy in the range of 300–1000 nm wavelength, the optical energy gap has been studied to address the effect of the existence of carbon nanotubes in the prepared samples. Using a homemade sensor system, the interaction of gases, including ammonia, nitrogen dioxide, and other organic odorants with the samples was investigated. Samples containing carbon nanotubes have exhibited better sensitivity and reversibility toward vapors, while zinc oxide only does not show reasonable performance at room temperature. The sensitivity toward nitrogen dioxide was found to be 96.6% for samples containing carbon nanotubes, while the sensitivity was 10.09% for samples of zinc oxide only.

Graphical Abstract

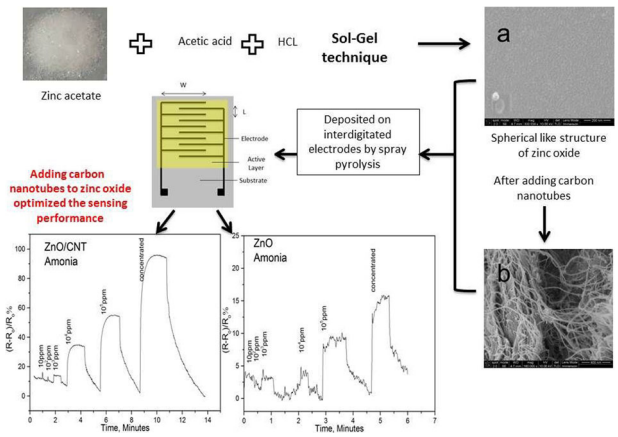

Keywords Zinc oxide · Sensors · Nanocomposite · Carbon nanotubes · Ammonia · Nitrogen dioxide

✉ Saad Abbas Jasim
saad.abbas1988@gmail.com

[1] Physics Department, College of Education for Pure Sciences, University of Babylon, Babylon, Iraq

[2] Department of Physics, College of Science, University of Babylon, Babylon, Iraq

[3] Medical physics Department, College of Technology and Health Sciences, Al-Mustaqbal University, Hillah, Babil 51001, Iraq

Published online: 15 September 2023

Highlights

- Composite of zinc oxide and carbon nanotubes was synthesized by sol-gel technique.
- Thin films have been deposited using spray pyrolysis method.
- Optical, SEM and FTIR confirmed the successful interaction between zinc oxide and carbon nanotubes.
- The composite materials show better sensitivity and response time towards odorants than bare zinc oxide.

1 Introduction

The most promising solid-state chemical sensors are conductometric metal oxide semiconductor thin films because of their compact size, low cost, low-power consumption, on-line operation, and great compatibility with microelectronic processing [1]. New sensing materials are being developed as a result of the rising demand for sensors that are highly selective, affordable, low-power, dependable, stable, and portable [2]. It has been discovered that the chemical components, surface state, morphology, and microstructure play significant roles in the performance of gas sensors. Different types of metal oxide, including zinc oxide, titanium dioxide, copper oxide, and others, have been developed and used in the fabrication of these sensors [3]. With an energy band gap of 3.3 eV and a 60 meV exciton binding energy, zinc oxide (ZnO) is regarded as one of the most promising semiconducting materials in recent years [4–6]. ZnO thin films have recently been investigated as thin film devices due to their promising electrical and optical properties along with strong thermal conductivity, high electron mobility, decent transparency, and other desirable properties, with a large excited binding energy and a wide and direct energy band gap in a room setting [7]. The broad research of this material as a gas sensor has been made possible by the recent advancement of doped and undoped ZnO films generated by diverse processes with the necessary gas sensitivity and selectivity of hydrocarbons, ammonia, oxygen, and nitrogen dioxide [8]. The structure of ZnO has a significant impact on the sensitivity and response time of the sensors. The polycrystalline zinc oxide material's gas-sensing characteristics are also noticeably influenced by the grain size. Experimental research has shown that as the mean grain size of ZnO sensors increases, their gas sensitivity reduces [9]. In addition, Due to its high exciton binding energy, zinc oxide is also a skilled material for short-wavelength optoelectronics, particularly for UV light-emitting devices and laser diodes (LDs) [10]. Developing ZnO in the nanostructure using a variety of techniques is fairly simple. Pulsed laser deposition (PLD) [11], magnetron sputtering [12], MOCVD [13], and the sol–gel process [14–16] are only a few of the techniques used to fully develop zinc oxide thin films. Although there are many ways to prepare zinc oxide, the sol-gel method is one of the most widely used methods for processing solutions to produce metal oxide nanoparticles because it produces thin films that are homogeneous and uniform and is effective because it produces very small nanoparticles on one side. Spray pyrolysis is one of the most practical wet processes for producing thin films, especially when employed with sol–gel prepared oxides. This technique does not require high quality targets, substrates, or vacuum at any point, which is a huge advantage if the technique is scaled up for industrial applications. By adjusting the spray parameters, it is simple to control the deposition rate and the thickness of the films over a wide range [5].

Contrarily, since their discovery, carbon nanotubes have attracted considerable interest due to their intriguing structural, mechanical, electronic, optical, and thermal properties as well as their excellent chemical stability, opening the door to potential high-technology applications like biosensors, supercapacitors, chemical electronic noses, and optoelectronic devices [17–22]. Carbon allotropes having a tube-shaped nanostructure are known as carbon nanotubes. They are frequently abbreviated as CNTs. It is possible to create nanotubes with a length-to-width ratio of up to 132,000,000:1. They possess outstanding qualities that present astounding prospects for the creation of novel materials and devices as it enhances the surface to volume ratio. A more valuable and advanced multifunctional material is created when CNTs are reinforced with the matrix material [23]. ZnO and CNTs work together to produce a variety of outstanding mechanical, electrical, and electromechanical capabilities that neither material could produce on its own. ZnO/CNT nanocomposite have received a lot of attention in recent years due to their exceptional qualities and wide range of potential uses. The outstanding characteristics of ZnO/CNTs nanocomposite have been enhanced using a variety of preparative techniques [24–26]. In addition, the foundation of carbon nanotubes increases the roughness of thin film which enhances the adsorption of contaminates in the sensing applications. The high surface area, in comparison to the volume of carbon nanotubes, increases the possible site that attracts strange molecules and physically interacts with them. This property is very important in gas-sensing application as it enhances the response and recovery of the device [21]. In this study, composites of ZnO and CNT were prepared using a modified sol–gel process for use in the detection of certain organic odorants. To determine the scope and characteristics of the species, including morphology, structure, and applications, a thorough analysis of the manufactured material was also examined.

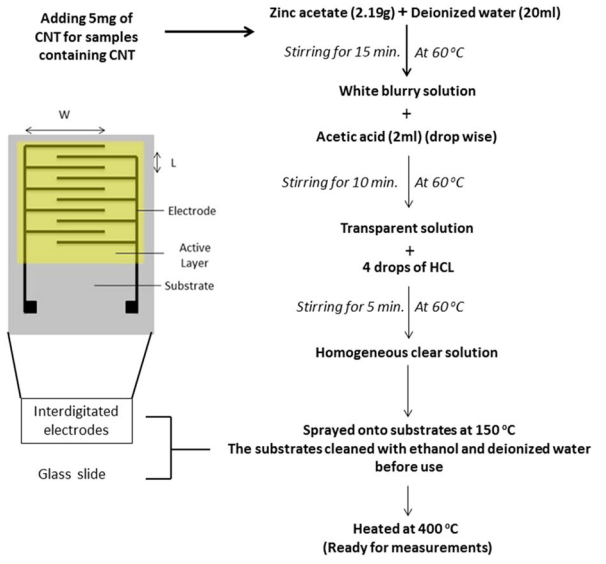

Fig. 1 Flowchart of the work and interdigitated electrodes made of gold. W the finger length, L distance between electrodes

2 Experimental

ZnO solution with a concentration of 0.5 M was prepared by dissolving zinc acetate (Zn(CH3COO)2) in (20 ml) of deionized water under stirring for 15 min, the color of the solution becomes white. Then slowly added 2 ml of acetic acid (CH3COOH) drop-wise with continuous stirring to this solution for (10 min), the color of the solution becomes transparent. Four drops of hydrochloric acid (HCl) were added and stirred for 5 min to obtain a homogeneous and clear solution. The temperature was kept at 60 °C while stirring. The mixture was then aged at room temperature for (24 h). To calculate the amount of zinc acetate to be dissolved, the following equation has been used [4]:

$$M = \left(\frac{W_t}{M_{\text{wt}}}\right)\left(\frac{1000}{v}\right) \quad (1)$$

where M is the molar concentration and equal to 0.5 M, W_t the amount of zinc acetate to be dissolved, M_{wt} the molecular weight of zinc acetate which is equal to (219.497 gm/mol), v the volume of deionized water.

All the materials and reagents used in this work have been supplied by Sigma-Aldrich and used as purchased without any further purification.

The same process was repeated with the enhanced sol–gel technique by the addition of 5 mg multi-walled carbon nanotubes with the solution prepared during the solution formation. Films were deposited using spray pyrolysis onto glass slides for optical and morphological properties and on interdigitated electrodes. Figure 1 represents the flowchart of the work and interdigitated electrodes

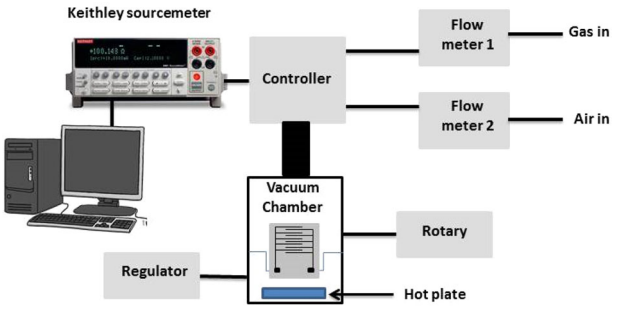

Fig. 2 The homemade experimental set up of gas-sensing measurement

used for sensing measurements. The temperature was kept at 150 °C during spraying. After deposition, films were heated at 400 °C at a programmable furnace. UV–Visible absorption spectra and energy gap calculations were recorded on Shimatzu doubled source light absorption spectrophotometer. The Fourier Transform Infrared technique has been employed to investigate the chemical functional groups of the prepared samples and the interaction between zinc oxide and carbon nanotubes. Morphology and energy dispersive of the prepared samples were explored using the field emission scanning electron microscopy (FESEM) technique. The experimental set-up for sensing measurements was built on the Keithley semiconductor characterization system (Fig. 2). Air was used as the diluent gas. Small amounts of contaminant have been transferred into 2 liters glass bottle using micro syringe and were left to vaporize. The vapor concentration was calculated according to the following gas law [21]:

$$c = \frac{22.4\rho T V_s}{273 M_{\text{wt}} V} \times 10^3 \quad (2)$$

where c is the concentration in ppm, ρ the density of the liquid sample in g/ml, T the temperature of container in Kelvin, V_s the volume of the liquid sample in µl, M_{wt} the molecular weight of sample in gm/mol, and V is the container volume in liter. The diluted gas has been further diluted by the two flow meters (Fig. 2) to obtain the following concentrations: 10, 10^2, 10^3, 10^4, and 10^5 ppm, which were then injected into the chamber by the rotary vacuum on the experiment set up. After exposure, fresh air was injected into the chamber to remove adsorbed molecules from the film surface.

3 Results and discussion

The UV–Visible absorption spectroscopy is one of the most crucial tools for examining the optical characteristics of nanoscale materials. Thin films double beam technique is used for this measurement. The reference slide was cleaned

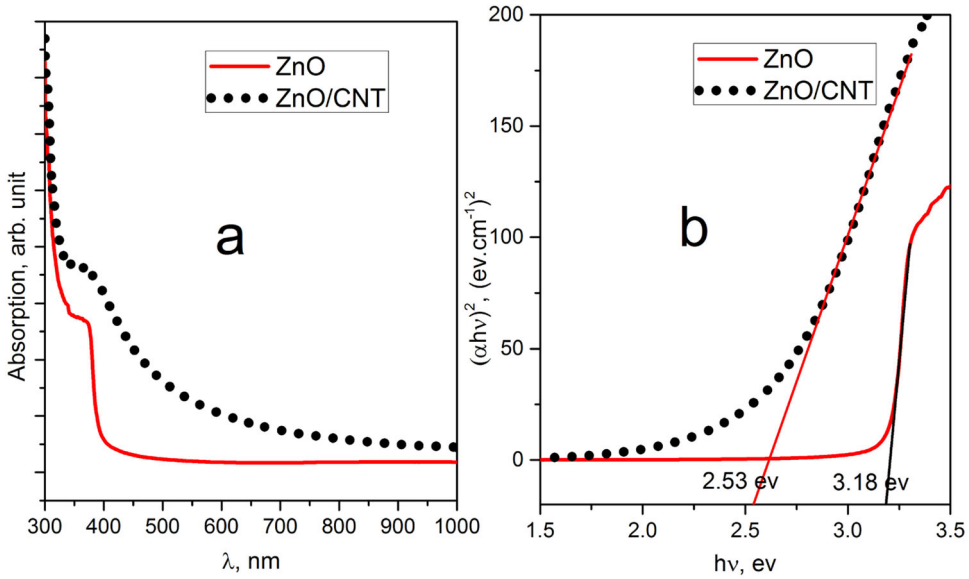

Fig. 3 **a** UV–visible absorption spectra of ZnO (solid lines) and ZnO/CNT hybrid (dashed lines) thin films annealed at 400 °C. **b** represents the Tauc's plot of photon energy

glass slide and the other beam was exposed onto the active layer. The absorbance spectra of the thin ZnO and ZnO/CNT hybrid films, which were annealed at 400 °C, are shown in Fig. 3 for the wavelength range of (300–1000) nm. It was discovered that the absorption was strong at 300 nm in the UV spectrum. The inherent electron transition between the valence band and conduction band is what causes this phenomena. Three hundred eighty nm was the location of additional exitonic bands because of the nanoscale particles. This peak was extremely visible (Fig. 3a), indicating that ZnO nanoparticles were successfully formed at this range of annealing temperature [27].

When CNTs are added to the samples, the absorption spectra undergo a red shift towards longer wavelength, which means lower energy is required to excite the electrons from higher occupied molecular orbitals to the lower unoccupied molecular orbitals, and hence lower energy gap is achieved. This finding shows that ZnO in the nanoscale has been successfully anchored to the side walls of the CNTs.

Since all curves have linear portions, the optical band gap (*Eg*) was computed using a Tauc plot, assuming a straight transition between the edge of the valence and conduction band [28]. The plot of $(\alpha h\nu)^2$ as a function of the energy of incident radiation ($h\nu$) has been shown in Fig. 3b. The energy band gap is obtained from the intercept of the extrapolated linear part of the curve with the energy axis and found to be; 3.18 and 2.53 eV for ZnO and ZnO/CNT samples respectively. The optical band gap (*Eg*) of samples containing CNT lowers, providing strong evidence of CNT presence. CNTs cause the band gaps of ZnO to become narrower, enabling improved absorption [24, 29]. The absorption band located in the visible wavelength is considered as the characteristic of the absorption of zinc oxide/carbon nanotubes nanocomposite, which indicates the foundation of new energy levels. Such difference in the absorption spectra is a sign of successful linked between the two materials. In addition, the existence of CNT in the matrix increased the charge transport and lowering the energy gap as CNT is one-dimensional electronic structure, conducts electrons and provides enhanced electron-hole pair production [30, 31].

The FTIR spectra of the ZnO and ZnO/CNT hybrid materials are displayed in Fig. 4. The acquired spectra clearly display the Zn-O absorption peak at a wavelength of around 540 cm^{-1}. According to the literature [24, 32–35], the O-H vibration extending from Zn-O-H types and C-H stretching vibration, respectively, are responsible for the absorption bands at 3450 and 2923 cm^{-1}. Because of an interaction between ZnO nanoparticles and the hydroxide group, the free O-H stretching bond at 3450 cm^{-1} is created. Carbon nanotubes may have been stretched carbon to carbon to produce the peak at 720 cm^{-1}, which only appeared in the spectra of the hybrid material [24]. This peak demonstrated that ZnO nanoparticle sidewall decoration of carbon nanotubes was successful.

Figure 5 shows images taken using scanning electron microscopy to examine the topography of the samples created for this project. Samples heated to 400 °C for 30 min demonstrated a spherical-type shape. ZnO grains are arranged uniformly in Fig. 4a at a nanoscale of about 20 nm or less. Depending on the method of manufacture, the coating, and the heat treatment, zinc oxide typically tends to create nano-sphere structures [36], rod-like structures [37], or nano-flower structures [38]. Figure 4b shows the SEM image of the samples containing CNT, which have shown clear tubes decorated by ZnO nanoparticles confirming the successful anchoring of the ZnO onto side-wall of the carbon nanotubes. This foundation was also reported elsewhere [39]. Figure 5c represents the high resolution of ZnO/CNT sample which

clearly showing the zinc oxide particles covering the carbon nanotubes. Figure 6 represents the EDS spectra of zinc oxide and zinc oxide-containing carbon nanotubes.

4 Gas detection

Using a homemade resistive sensor device, samples were exposed to ammonia and nitrogen dioxide at a concentration of 10, 10^2, 10^3, 10^4, 10^5 ppm and concentrated gas at room temperature. Due to its low-power consumption and long-lasting stability, gas sensors with very high responsiveness to odorants and working at room temperature are viewed as more desirable gadgets [40]. Zinc oxide, a semiconducting oxide, is now a well-known candidate for a resistance-based gas sensor. However, its vast applications in the field of real-time gas detection, particularly in flammable and volatile gas environments, become limited by its higher working temperature. Global research efforts were made in this competition to lower the temperature at which the sensor device was operating, and literature [41] has thoroughly evaluated the room temperature gas-sensing capabilities of ZnO. In general, doping with other materials, morphological enhancements, and light initiations are the most successful methods for producing room-temperature gas detection of ZnO-based gas sensors. Finally, some ideas for further research on tools for room-temperature gas detection are considered [42].

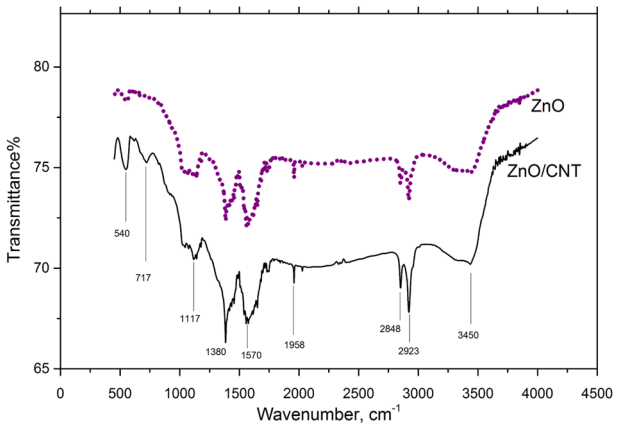

Fig. 4 The FTIR spectra of ZnO and ZnO/CNT prepared by sol–gel method

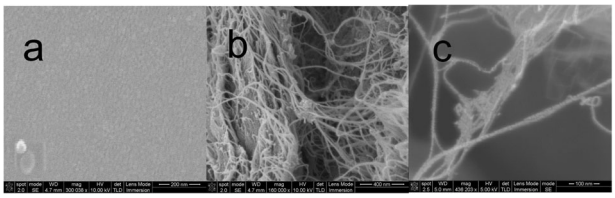

Fig. 5 SEM images of sprayed ZnO thin films prepared by sol–gel and annealed at 400 °C; **a** ZnO, **b** ZnO/CNT and **c** High magnification of (**c**) showing the particles of ZnO nicely decorating the tubes

Figure 7 displays the ZnO and hybrid films' reactivity over time to ammonia and nitrogen dioxide. Since the resistance has not returned to its initial value after the gas has been expelled from the sample surface, it is clear that ZnO does not exhibit any discernible response and is not reversible. The non-recoverable device is suggested to take place because of the diffusion of the gas molecule inside the films where no sites existed for physisorption between film and analyte molecule. The hybrid film, on the other hand, has demonstrated rather fascinating behavior as a result of gas interaction, making them an attractive candidate for sensing applications. The diffusion of gas molecules inside the composite film is anticipated to be inhibited by the presence of CNT, and the majority of interaction is predicted to occur at the film's surface [43]. Carbon nanotubes are p-doped in the room temperature as a sequence of oxygen physisorption. Therefore, the hole conductivity increases after exposure to further p-type analyte and thus,

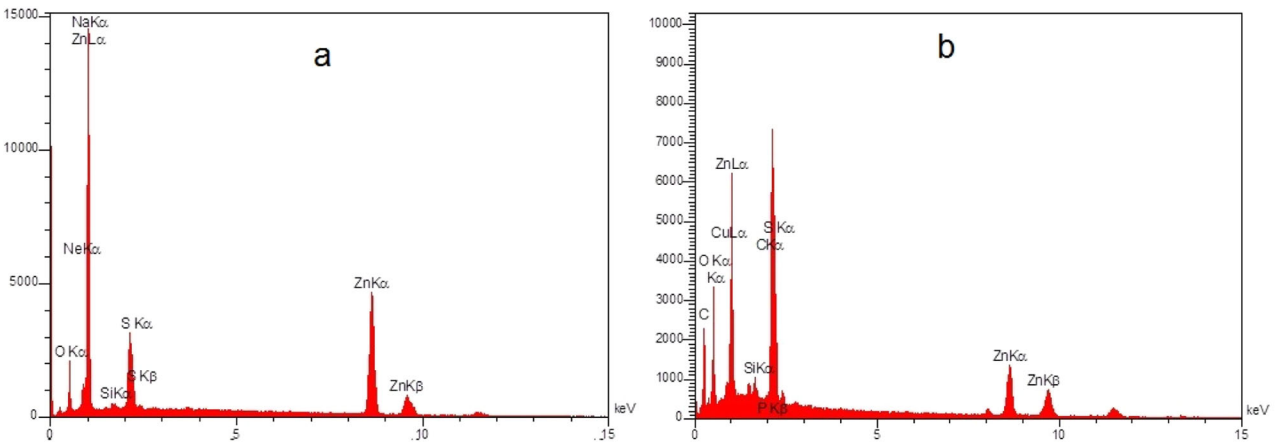

Fig. 6 EDS spectra of spun ZnO thin films prepared by sol–gel and annealed at 400 °C; **a** ZnO, **b** ZnO/CNT

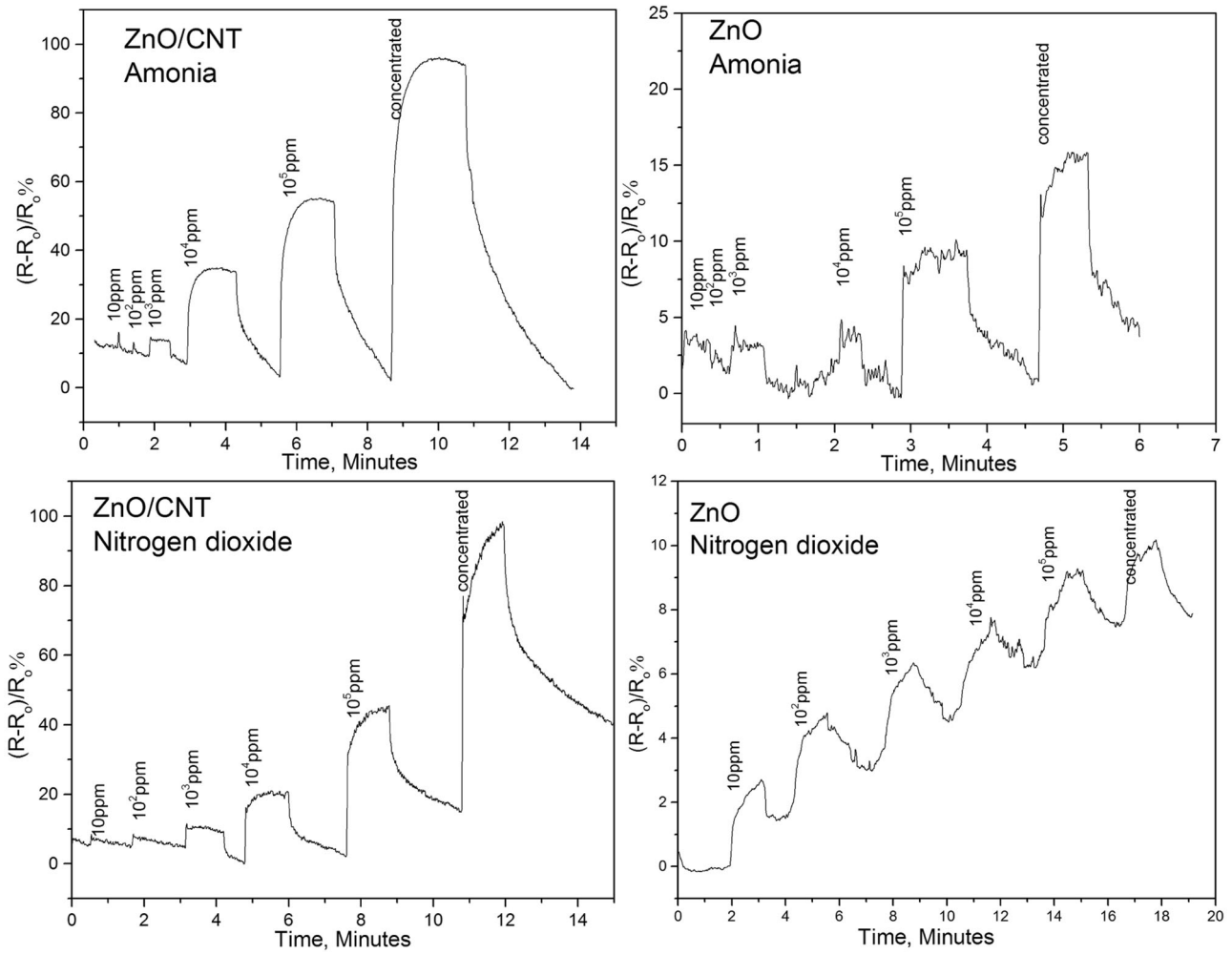

Fig. 7 Time dependence of the response ($R\% = R - R_o/R_o{*}100\%$) for ZnO and ZnO/CNT films upon exposure to ammonia and nitrogen dioxide vapors

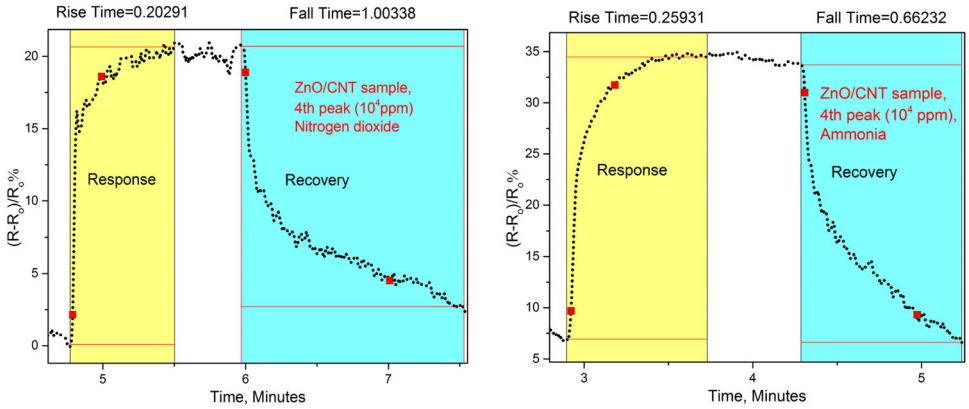

Fig. 8 The response and recovery times of ZnO/CNT due to ammonia and nitrogen dioxide taken at concentration of 10^4 ppm

the resistivity decreases. Furthermore, contaminant molecule can also promote the degradation of the sidewalls of the tubs. In particular, the chemisorption of nitrogen dioxide due the nitro groups and nitrite groups was recognized as probable sensing mechanisms [44, 45].

The computed response and recovery periods, which were determined by fitting the 4th peaks with rise and fall times which were 90% of the maximum response after gas on and 90% of the return to the original state after gas off. Figure 8 shows the fitting curves for ZnO/CNT devices responding to

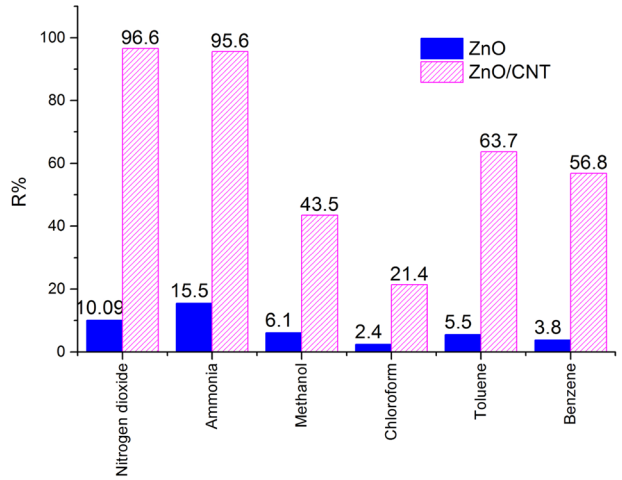

Fig. 9 The responses of ZnO and ZnO/CNT devices toward some volatile gases (concentrated)

Table 1 Response and recovery times for ZnO/CNT device toward different vapors

Vapor	Response time (s)	Recovery time (s)
Nitrogen dioxide	12.17	60.20
Ammonia	15.54	39.73
Methanol	24.39	176.85
Chloroform	62.22	201.09
Toluene	19.43	88.87
Benzene	37.64	90.05

ammonia and nitrogen dioxide at the concentrations of 10^4ppm. For comparison, the samples have been exposed to different gasses, including methanol, chloroform, toluene, and benzene. The responses were summarized in Fig. 9, and the higher response was found to be due to exposure to ammonia and nitrogen dioxide vapors. The response and recovery times were calculated for samples containing carbon nanotubes only as were no clear recovery in the device synthesized form only ZnO. The values of response and recovery times are concluded in Table 1.

5 Conclusion

By using sol–gel and spray pyrolysis procedures, thin films of zinc oxide and a hybrid of zinc oxide and carbon nanotubes have been produced. The optical band gap is reduced by around 1 ev as a result of carbon nanotubes, according to the UV–visible absorption spectra. According to the SEM images, the synthesized zinc oxide's grain size was about 20 nm. The produced ZnO/CNT showed a very clear interaction as the FTIR exhibited. The interaction of ammonia and nitrogen dioxide gases with the synthesized devices has been investigated, and the findings indicate that the presence of carbon nanotubes lowers the chemical interaction, leading to complete recovery after purging the samples with fresh air. The higher sensitivity found due to nitrogen dioxide was 96.6% followed by ammonia of about 95.6%. The calculation revealed that the response times were 12.17 and 15.54 s, and the recovery times were 60.20 and 39.73 s for nitrogen dioxide and ammonia, respectively. The mixed gas measurements were not applicable in this work as the sensitivity towards ammonia and nitrogen dioxide are convergent; therefore, it was quite difficult to separate between the two gases. It is suggested that manipulating the carbon nanotubes ratio and/or use of graphene oxide in the future work to enhance the selectivity of the prepared devices. Another future enhancement is that using different interdigitated electrodes mask with more fingers to reduce the resistivity and hence improve the response.

Acknowledgements The author would like to acknowledge the provision of instruments and necessary materials by (1) Department of Physics, College of Science, University of Babylon, (2) Department of Physics, College of Education for pure Sciences, University of Babylon, and (3) Medical physics Department, College of Technology and Health Sciences, Al-Mustaqbal University, to help in completing this work.

Author contributions The contribution of the authors is as follows: SAJ and HAJB wrote the main manuscript and prepared all of the samples for testing; the remaining authors prepared the figures and discussed the main results, and made a review for the work.

Compliance with ethical standards

Conflict of interest The authors declare no competing interests.

References

1. Wang ZL (2004) J Phys Condens Matter 16:R829
2. Leonardi SG (2017) Chemosensors 5:17
3. Wang C, Yin L, Zhang L, Xiang D, Gao R (2010) Sensors 10:2088
4. Xu L, Li X, Chen Y, Xu F (2011) Appl Surf Sci 257:4031
5. Kadem B, Banimuslem HA, Hassan A (2017) Karbala Int J Mod Sci 3:103
6. Deng G, Zhang Y, Yu Y, Han X, Wang Y, Shi Z, Dong X, Zhang B, Du G, Liu Y (2020) ACS Appl Mater Interfaces 12:6788
7. Wang ZL (2004) Mater Today 7:26
8. Martins R, Fortunato E, Nunes P, Ferreira I, Marques A, Bender M, Katsarakis N, Cimalla V, Kiriakidis G (2004) J Appl Phys 96:1398
9. Roy S, Basu S (2002) Bull Mater Sci 25:513
10. Lieber CM (1998) Solid State Commun 107:607
11. Alamro FS, Toghan A, Ahmed HA, Mostafa AM, Alakhras AI, Mwafy EA (2022) Microsc Res Tech 85:1611
12. Ondo-Ndong R, Essone-Obame H, Moussambi ZH, Koumba N (2018) J Theor Appl Phys 12:309

13. Saravade VG, Manzoor Z, Corda AM, Zhou C, Ferguson IT, Lu L (2020) In: Proc. SPIE 11288, quantum sensing and nano electronics and photonics, p 112881X–1
14. Natsume Y, Sakata H (2000) Thin Solid Films 372:30
15. Li H, Wang J, Liu H, Zhang H, Li X (2005) J Cryst Growth 275:e943
16. Ismail AM, Menazea AA, Kabary HA, El-Sherbiny AE, Samy A (2019) J Mol Struct 1196:332
17. Komatsubara K, Suzuki H, Inoue H, Kishibuchi M, Takahashi S, Marui T, Umezawa S, Nakagawa T, Nasu K, Maetani M, Tanaka Y (2022) ACS Appl Nano Mater 5:1
18. Shooshtari M, Salehi A (2022) Sens Actuators B Chem 357:131418
19. Snow ES, Perkins FK, Robinsona JA (2006) Chem Soc Rev 35:790
20. Banimuslem H, Hassan A, Basova T, Durmus M, Tuncel S, Esenpinar AA, Gürek AG, Ahsen V (2015) J Nanosci Nanotechnol 15:2157
21. Banimuslem H, Hassan A, Basova T, Esenpinar AA, Tuncel S, Durmuş M, Gürek AG, Ahsen V (2015) Sens Actuators B Chem 207:224
22. Avouris P, Freitag M, Perebeinos V (2008) Nat Photonics 2:341
23. Krueger A (2010) Carbon materials and nanotechnology. Wiley Online Publisher, USA
24. Mohamed MM, Ghanem MA, Khairy M, Naguib E, Alotaibi NH (2019) Appl Surf Sci 487:539
25. Kumar S, Ahlawat W, Kumar R, Dilbaghi N (2015) Biosens Bioelectron 70:498
26. Phin HY, Ong YT, Sin JC (2020) J Environ Chem Eng 8:103222
27. Hammad TM, Salem JK, Harrison RG (2010) Superlattices Microstruct 47:335
28. Coulter JB, Birnie DP (2018) Phys Status Solidi Basic Res 255:1700393
29. Das Mulmi D, Dhakal A, Shah BR (2015) Nepal J Sci Technol 15:111
30. Chen L, Yi-Ching H, Wei-Sheng G, Chao-Ming H, Ting-Chung P (2009) Electrochim Acta 54:15
31. Mokhtar M, Ghanem M, Khairy M, Naguib E, Alotaibi N (2019) Appl Surf Sci 487:1–1420
32. Thareja RK, Shukla S (2007) Appl Surf Sci 253:8889
33. Kulkarni SS, Sawarkar Mahavidyalaya S, Shirsat MD (2015) Int J Adv Res Phys Sci 2:14
34. Jurablu S, Farahmandjou M, Firoozabadi TP (2015) J Sci Islam Repub Iran 26:281
35. Balogun SW, James OO, Sanusi YK, Olayinka OH (2020) SN Appl Sci 2:1
36. Tetrycz H, Byrczek M, Rac O (2010) In: Proc. 2010 international students and young scientists workshop photonics and microsystems, STYSW 2010, p 7–9
37. Vergés MA, Mifsud A, Serna CJ (1990) J Chem Soc Faraday Trans 86:959
38. Pachauri V, Subramaniam C, Pradeep T (2006) Chem Phys Lett 423:240
39. Abussaud BA (2021) Sustainability 13:11716
40. Zhu L, Zeng W (2017) Sens Actuators A Phys 267:242
41. Zhu L, Li Y, Zeng W (2018) Appl Surf Sci 427:281
42. Kumar R, Al-Dossary O, Kumar G, Umar A (2015) NanoMicro Lett 7:97
43. Banimuslem H, Hassan A, Basova T, Yushina I, Durmus M, Tuncel S, Esenpinar AA, Gürek AG, Ahsen V (2014) Key Eng Mater 605:461–464
44. Schroeder V, Suchol S, Maggie H, Sibo L, Timothy S (2018) Chem Rev 119:1
45. Zhang Y, Suc C, Liu Z, Li J (2006) J Phys Chem B 110:45